Frontiers of Information Technology & Electronic Engineering
www.zju.edu.cn/jzus; engineering.cae.cn; www.springerlink.com
ISSN 2095-9184 (print); ISSN 2095-9230 (online)
E-mail: jzus@zju.edu.cn

Optimal precoding for full-duplex base stations under strongly correlated self-interference channels*

Jun WANG[1,2], Xiao-jie WEN[2], Chuan HUANG‡[2,3], Chao-jin QING[2,4]

([1]*College of Electrical and Information Engineering, Southwest University for Nationalities, Chengdu 610041, China*)

([2]*Beijing Institute of Satellite Information Engineering, Beijing 100086, China*)

([3]*National Key Laboratory of Science and Technology on Communications, University of Electronic Science and Technology of China, Chengdu 611731, China*)

([4]*School of Electrical and Information Engineering, Xihua University, Chengdu 610039, China*)

E-mail: 13880458609@139.com; ziwen7189@aliyun.com; huangch@uestc.edu.cn; qingchj@uestc.edu.cn

Received Jan. 9, 2017; Revision accepted Apr. 6, 2017; Crosschecked May 30, 2017

Abstract: We study the optimal precoding for a full-duplex (FD) system, where one FD multi-antenna base station (BS) respectively transmits to and receives from two half-duplex single-antenna mobile users (MUs) on the same time slot and frequency band. At the FD BS, the received signal from the desired MU is severely affected by the extremely strong self-interference (SI) from its transmit antennas to the receive antennas. In the presence of residual SI after imperfect SI cancellation, the downlink transmission rate maximization problem subject to a targeted uplink rate is formulated as a non-convex optimization problem to characterize the achievable rate region for the considered system. Considering the case in which the SI channel is strongly correlated, the above problem is transformed into a convex problem by exploiting the rank-one property of the SI channel, which can be solved efficiently. Finally, numerical results validate the effectiveness of the proposed scheme.

Key words: Linear precoding; Full-duplex; Achievable rate region; Strongly correlated self-interference channel
http://dx.doi.org/10.1631/FITEE.1700022 **CLC number:** TN92

1 Introduction

Full-duplex (FD) radios, which simultaneously transmit and receive on the same frequency, can potentially double the spectral efficiency compared with the conventional half-duplex (HD) ones (e.g., frequency division duplexing (FDD) or time division duplexing (TDD) radios), for which two orthogonal channels are respectively allocated for transmission and reception (Cirik *et al.*, 2014; Sabharwal *et al.*, 2014). However, it is difficult to completely remove severe self-interference (SI) between the transmit (Tx) and receive (Rx) antennas at the FD radio by using the existing SI cancellation methods, and the residual SI may significantly degrade the system performance (Sabharwal *et al.*, 2014).

In the presence of residual SI, linear precoding was studied for the FD cellular systems, to balance the SI suppression and the data transmissions for both the uplink (UL) and downlink (DL) channels (Nguyen *et al.*, 2013; 2014; Cirik, 2015; Huberman and Le-Ngoc, 2015). With perfect channel state information (CSI) available at both the base station (BS) and mobile users (MUs), Nguyen *et al.* (2013; 2014) developed precoding algorithms to maximize the sum rate of the UL and DL channels separately for the cases with and without the co-channel interference from the UL MU to its DL counterpart. Due

‡ Corresponding author

* Project supported by the National Natural Science Foundation of China (Nos. 61401030 and 61501093)

ORCID: Chuan HUANG, http://orcid.org/0000-0001-5965-0823

to the non-convexity of the sum rate maximization problems, sequential convex approximation (SCA) based methods were adopted and only local optimal solutions were obtained (Nguyen *et al.*, 2013; 2014).

For the case with imperfect CSI of the SI channel, a non-convex sum rate maximization problem was formulated, and two sub-optimal precoding algorithms based on sequential convex programming (SCP) and sequential convex approximation for matrix-variable programming (SCAMP) were proposed (Huberman and Le-Ngoc, 2015). Moreover, Cirik (2015) considered the SI channel with imperfect CSI and modeled the nonlinearities and phase noises at the transmitters and receivers as Gaussians. Then a gradient projection method was developed to approximately solve the non-convex proportional fairness (PF) based optimization problem, which yielded a near-maximum sum rate of the UL and DL channels (Cirik, 2015).

To sum up, the existing research on precoding design for the FD cellular system focuses mainly on the general SI channel case, which leads to non-convex optimization problems, and the obtained precoding schemes achieve only sub-optimal performance. Since the relative positions between the transmit and receive antennas of the FD transceiver are fixed, the correlations between the multiple-input multiple-output (MIMO) SI channels of the FD transceiver are fixed, and can be deduced at the beginning. Therefore, given a specific antenna placement, the correlations between the MIMO SI channels can be used as prior knowledge to design a more efficient precoding scheme. As a commonly existing scenario in short-range communications, we consider the case in which the SI channel is strongly correlated, i.e., the SI channel matrix is of rank one. Haneda *et al.* (2013a; 2013b) pointed out that the MIMO channel matrix was a rank-one matrix in a single-polarized line-of-sight (LoS) scenario, where the Tx and Rx arrays were with different polarizations. Furthermore, in the case that the Tx and Rx arrays had the same polarization, Pu *et al.* (2015) showed that the MIMO channel matrix in short-range communications was approximatively of rank one when the elevation angle of the Rx array was small or any one of the azimuth angles of Tx and Rx arrays was almost $\pi/2$, assuming that the Tx array and the center of the Rx array lay in the xy-plane. Then we propose a precoding scheme, which is claimed to achieve the optimal performance by exploiting the strong correlation of the SI channel. For the purpose of exposition, a simple system with one FD multi-antenna BS and two HD single-antenna MUs is considered. First, the DL rate maximization problem subject to a targeted UL rate is formulated as a non-convex optimization problem to characterize the achievable rate region for the considered system. In the considered scenario of the rank-one SI channel matrix, the above optimization problem is transformed into a convex problem, which can be solved by standard convex optimization tools. Moreover, the proposed scheme is applied to the general SI channel case with proper approximation to the SI channel. By analysis and simulation, the proposed scheme is validated to be effective to characterize the achievable rate region for the considered system.

Notations: $\boldsymbol{H}^{\mathrm{T}}$, $\boldsymbol{H}^{*}$, $\boldsymbol{H}^{\mathrm{H}}$, $\mathrm{tr}(\boldsymbol{H})$, $|\boldsymbol{H}|$, and $\|\boldsymbol{H}\|$ denote the transpose, conjugate, conjugate transpose, trace, determinant, and Frobenius norm of matrix $\boldsymbol{H}$, respectively. $\boldsymbol{H} \succeq 0$ means that $\boldsymbol{H}$ is a positive semi-definite matrix. In addition, we define 'log' to be base-2.

2 System model

As shown in Fig. 1, we consider a single cell cellular system, which consists of one FD BS equipped with multiple antennas and two HD MUs each with one antenna. The FD BS transmits to the DL MU (S_{d}) and receives from the UL MU (S_{u}) at the same time and frequency slots. Similar to Nguyen *et al.*

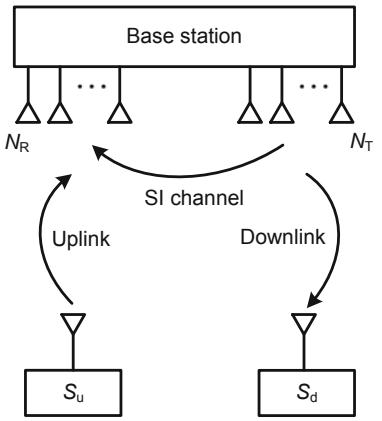

Fig. 1 A single cell cellular system consisting of one full-duplex base station with multiple antennas and two half-duplex mobile users each with one antenna

(2013), the co-channel interference from the UL to DL MUs is ignored due to the relatively long distance between the two MUs. The BS can simultaneously transmit and receive by shared antennas with circulators or by separated antennas (Bharadia *et al.*, 2013). Taking the case with separated antennas as an example, the numbers of Tx and Rx antennas are denoted as N_{T} and N_{R}, respectively.

By applying linear precoding at the BS, the received signal y_{d} at the DL MU (S_{d}) is given as follows:

$$y_{\mathrm{d}} = \boldsymbol{h}_{\mathrm{d}}^{\mathrm{T}} \boldsymbol{W}_{\mathrm{d}} \boldsymbol{s}_{\mathrm{d}} + n_{\mathrm{d}}, \tag{1}$$

where $\boldsymbol{h}_{\mathrm{d}} \in \mathbb{C}^{N_{\mathrm{T}} \times 1}$ represents the DL channel, $\boldsymbol{W}_{\mathrm{d}} \in \mathbb{C}^{N_{\mathrm{T}} \times N_{\mathrm{T}}}$ is the linear precoding matrix at the BS, $\boldsymbol{s}_{\mathrm{d}} \in \mathbb{C}^{N_{\mathrm{T}} \times 1}$ denotes the signal transmitted from the BS to S_{d}, and n_{d} is the circularly symmetric complex Gaussian (CSCG) noise with zero mean and variance N_0.

Without loss of generality, the elements of $\boldsymbol{s}_{\mathrm{d}}$ are assumed to be independent of each other, i.e., $\mathbb{E}[\boldsymbol{s}_{\mathrm{d}} \boldsymbol{s}_{\mathrm{d}}^{\mathrm{H}}] = \boldsymbol{I}_{N_{\mathrm{T}}}$, and perfect CSI (even if the SI channel at the BS is perfectly known, the SI cannot be completely cancelled due to the quantization errors of analog-to-digital converters (ADCs) (Sabharwal *et al.*, 2014)) is available at both the BS and S_{d}. Then the maximum transmission rate R_{d} of the DL channel is given as follows (Nguyen *et al.*, 2013):

$$R_{\mathrm{d}} = \log\left(1 + \boldsymbol{h}_{\mathrm{d}}^{\mathrm{T}} \boldsymbol{Q}_{\mathrm{d}} \boldsymbol{h}_{\mathrm{d}}^{*} / N_0\right), \tag{2}$$

where $\boldsymbol{Q}_{\mathrm{d}} = \boldsymbol{W}_{\mathrm{d}} \boldsymbol{W}_{\mathrm{d}}^{\mathrm{H}}$ represents the precoding covariance matrix, and $\mathrm{tr}(\boldsymbol{Q}_{\mathrm{d}}) \le P_{\mathrm{d}}$ with P_{d} being the power budget of the BS.

By applying the Cauchy-Schwarz inequality, it follows

$$\boldsymbol{h}_{\mathrm{d}}^{\mathrm{T}} \boldsymbol{W}_{\mathrm{d}} \boldsymbol{W}_{\mathrm{d}}^{\mathrm{H}} \boldsymbol{h}_{\mathrm{d}}^{*} \le \|\boldsymbol{h}_{\mathrm{d}}\|^2 \sum_{i=1}^{N_{\mathrm{T}}} \|\boldsymbol{w}_i\|^2, \tag{3}$$

where $\boldsymbol{w}_i$ is the ith column vector of $\boldsymbol{W}_{\mathrm{d}}$. As a result, the upper bound on the maximum DL transmission rate is given as

$$R_{\mathrm{d}}^{\mathrm{U}} = \log\left(1 + P_{\mathrm{d}} \|\boldsymbol{h}_{\mathrm{d}}\|^2 / N_0\right). \tag{4}$$

Similarly, the received signal $\boldsymbol{y}_{\mathrm{u}} \in \mathbb{C}^{N_{\mathrm{R}} \times 1}$ at the BS is given as

$$\boldsymbol{y}_{\mathrm{u}} = \boldsymbol{h}_{\mathrm{u}} s_{\mathrm{u}} + \boldsymbol{H}_{\mathrm{s}} \boldsymbol{W}_{\mathrm{d}} \boldsymbol{s}_{\mathrm{d}} + \boldsymbol{n}_{\mathrm{u}}, \tag{5}$$

where $\boldsymbol{h}_{\mathrm{u}} \in \mathbb{C}^{N_{\mathrm{R}} \times 1}$ represents the UL channel, s_{u} is the signal from S_{u}, $\boldsymbol{H}_{\mathrm{s}} \in \mathbb{C}^{N_{\mathrm{R}} \times N_{\mathrm{T}}}$ is the channel matrix of the residual SI after imperfect SI cancellation at the BS, and $\boldsymbol{n}_{\mathrm{u}}$ is the CSCG noise satisfying $\boldsymbol{n}_{\mathrm{u}} \sim \mathcal{CN}(0, N_0 \boldsymbol{I}_{N_{\mathrm{R}}})$.

In general, the residual SI is non-Gaussian, while Gaussian distributed SI provides a lower bound on the achievable rate for the UL transmission to characterize the UL performance (Nguyen *et al.*, 2013; Cirik *et al.*, 2014). Therefore, the maximum transmission rate R_{u} of the UL channel can be computed as follows (Nguyen *et al.*, 2013):

$$R_{\mathrm{u}} = \log\left|\boldsymbol{I} + P_{\mathrm{u}} (N_0 \boldsymbol{I} + \boldsymbol{H}_{\mathrm{s}} \boldsymbol{Q}_{\mathrm{d}} \boldsymbol{H}_{\mathrm{s}}^{\mathrm{H}})^{-1} \boldsymbol{h}_{\mathrm{u}} \boldsymbol{h}_{\mathrm{u}}^{\mathrm{H}}\right|, \tag{6}$$

where $P_{\mathrm{u}} = \mathbb{E}[s_{\mathrm{u}} s_{\mathrm{u}}^{*}]$ is the transmit power at S_{u}.

3 Characterization of the achievable rate region

In this section, we discuss the achievable rate region for the considered system, which characterizes the optimal performance of the corresponding UL and DL channels. The achievable rate region is defined as follows (Zhang *et al.*, 2009):

$$\mathcal{R}(P_{\mathrm{d}}) \triangleq \bigcup_{\mathrm{tr}(\boldsymbol{Q}_{\mathrm{d}}) \le P_{\mathrm{d}}} \{(r_{\mathrm{u}}, r_{\mathrm{d}}) | r_{\mathrm{u}} \le R_{\mathrm{u}}, r_{\mathrm{d}} \le R_{\mathrm{d}}\}, \tag{7}$$

where r_{u} and r_{d} represent the achievable rates of the UL and DL channels, respectively.

3.1 General self-interference channel case

A commonly adopted method to find all the rate pairs on the boundary of the achievable rate region defined in Eq. (7) is to maximize the rate of the DL channel subject to a targeted rate of the UL channel, i.e.,

$$\begin{aligned} &(\mathrm{P1}) \ \max_{\{\boldsymbol{Q}_{\mathrm{d}}\}} \ R_{\mathrm{d}} \\ &\text{s.t.} \ \ R_{\mathrm{u}} \ge \alpha, \ \mathrm{tr}\,(\boldsymbol{Q}_{\mathrm{d}}) \le P_{\mathrm{d}}, \ \boldsymbol{Q}_{\mathrm{d}} \succeq 0, \end{aligned} \tag{8}$$

where $\alpha \ge 0$ is a constant denoting the targeted rate of the UL channel. The goal of Problem (P1) is to maximize the rate of the DL channel under the conditions in which the rate of the UL channel is not less than α and the maximum transmit power of the BS is P_{d}.

Denote β as the optimal solution to Problem (P1) under a given α, and (α, β) is thus one rate pair on the boundary of the desired achievable rate

region. As a result, all the rate pairs on the boundary of the achievable rate region can be calculated by solving Problem (P1) with different α's. However, by substituting Eqs. (2) and (6) into Eq. (8), Problem (P1) is proved to be non-convex in general (Boyd and Vandenberghe, 2004), and thus its globally optimal solution cannot be found efficiently.

3.2 Strongly correlated self-interference channel case

In this subsection, Problem (P1) is further analyzed under the case in which the SI channel is strongly correlated, i.e., the matrix $\boldsymbol{H}_{\mathrm{s}}$ is of rank one. In this case, the singular-value-decomposition (SVD) of $\boldsymbol{H}_{\mathrm{s}}$ can be expressed as follows (Yousif *et al.*, 2015):

$$\boldsymbol{H}_{\mathrm{s}}=\lambda \boldsymbol{u}_{\mathrm{s}}\boldsymbol{v}_{\mathrm{s}}^{\mathrm{H}}, \tag{9}$$

where both $\boldsymbol{u}_{\mathrm{s}}$ and $\boldsymbol{v}_{\mathrm{s}}$ are complex-valued unit vectors, and $\lambda>0$ is the non-zero singular value of $\boldsymbol{H}_{\mathrm{s}}$. We then have the following proposition:

Proposition 1 With a rank-one SI channel matrix $\boldsymbol{H}_{\mathrm{s}}$, the maximum UL transmission rate given in Eq. (6) is simplified as

$$\begin{aligned}R_{\mathrm{u}}=\log\Bigg[&1+\frac{P_{\mathrm{u}}}{N_0+\lambda^2\boldsymbol{v}_{\mathrm{s}}^{\mathrm{H}}\boldsymbol{Q}_{\mathrm{d}}\boldsymbol{v}_{\mathrm{s}}}\boldsymbol{h}_{\mathrm{u}}^{\mathrm{H}}\left(\boldsymbol{u}_{\mathrm{s}}\boldsymbol{u}_{\mathrm{s}}^{\mathrm{H}}\right)\boldsymbol{h}_{\mathrm{u}}\\&+\frac{P_{\mathrm{u}}}{N_0}\boldsymbol{h}_{\mathrm{u}}^{\mathrm{H}}\left(\boldsymbol{I}-\boldsymbol{u}_{\mathrm{s}}\boldsymbol{u}_{\mathrm{s}}^{\mathrm{H}}\right)\boldsymbol{h}_{\mathrm{u}}\Bigg].\end{aligned} \tag{10}$$

The proof is given in Appendix A.

Since $\boldsymbol{Q}_{\mathrm{d}}\succeq 0$, it follows $\boldsymbol{v}_{\mathrm{s}}^{\mathrm{H}}\boldsymbol{Q}_{\mathrm{d}}\boldsymbol{v}_{\mathrm{s}}\geq 0$. Then the upper and lower bounds on the maximum UL transmission rate are respectively computed as

$$R_{\mathrm{u}}^{\mathrm{U}}=\log(1+P_{\mathrm{u}}\|\boldsymbol{h}_{\mathrm{u}}\|^2/N_0), \tag{11}$$

$$R_{\mathrm{u}}^{\mathrm{L}}=\log\left[1+\frac{P_{\mathrm{u}}}{N_0}\boldsymbol{h}_{\mathrm{u}}^{\mathrm{H}}(\boldsymbol{I}-\boldsymbol{u}_{\mathrm{s}}\boldsymbol{u}_{\mathrm{s}}^{\mathrm{H}})\boldsymbol{h}_{\mathrm{u}}\right], \tag{12}$$

with $\boldsymbol{v}_{\mathrm{s}}^{\mathrm{H}}\boldsymbol{Q}_{\mathrm{d}}\boldsymbol{v}_{\mathrm{s}}$ being equal to 0 or infinity.

Based on Proposition 1, the design of the variable in Problem (P1) can be simplified. First, a new matrix $\boldsymbol{G}=[\boldsymbol{h}_{\mathrm{d}}^{*},\boldsymbol{v}_{\mathrm{s}}]$ is introduced, whose SVD is given as follows (Yousif *et al.*, 2015):

$$\boldsymbol{G}=\boldsymbol{U}\boldsymbol{\Sigma}\boldsymbol{V}^{\mathrm{H}}, \tag{13}$$

where $\boldsymbol{U}\in\mathbb{C}^{N_{\mathrm{T}}\times 2}$, $\boldsymbol{\Sigma}=\mathrm{diag}(\sigma_1,\sigma_2)$, and $\boldsymbol{V}\in\mathbb{C}^{2\times 2}$. Then we can show the simplified structure of the optimal precoding covariance matrix $\boldsymbol{Q}_{\mathrm{d}}$.

Proposition 2 With a rank-one SI channel matrix $\boldsymbol{H}_{\mathrm{s}}$, the optimal precoding covariance matrix $\boldsymbol{Q}_{\mathrm{d}}$ for Problem (P1) has the following structure:

$$\boldsymbol{Q}_{\mathrm{d}}=\boldsymbol{U}\boldsymbol{B}\boldsymbol{U}^{\mathrm{H}}, \tag{14}$$

where $\boldsymbol{B}\in\mathbb{C}^{2\times 2}$.

The proof is given in Appendix B.

Remark 1 Given that $\boldsymbol{U}$ represents a subspace generated by vectors $\boldsymbol{h}_{\mathrm{d}}^{*}$ and $\boldsymbol{v}_{\mathrm{s}}$, Proposition 2 reveals that the optimal precoding at the BS depends only on the DL and SI channels. The reason is that the optimal precoding at the BS is designed to ensure the DL transmission as well as to suppress the residual SI.

With Propositions 1 and 2, Problem (P1) is simplified as

$$\begin{aligned}(\mathrm{P2})\ &\max_{\{\boldsymbol{B}\}}\ \log\left(1+\hat{\boldsymbol{h}}_{\mathrm{d}}^{\mathrm{H}}\boldsymbol{B}\hat{\boldsymbol{h}}_{\mathrm{d}}/N_0\right)\\ \mathrm{s.t.}\ &\log\Bigg[1+\frac{P_{\mathrm{u}}}{N_0+\lambda^2\hat{\boldsymbol{v}}_{\mathrm{s}}^{\mathrm{H}}\boldsymbol{B}\hat{\boldsymbol{v}}_{\mathrm{s}}}\boldsymbol{h}_{\mathrm{u}}^{\mathrm{H}}\left(\boldsymbol{u}_{\mathrm{s}}\boldsymbol{u}_{\mathrm{s}}^{\mathrm{H}}\right)\boldsymbol{h}_{\mathrm{u}}\\&\quad+\frac{P_{\mathrm{u}}}{N_0}\boldsymbol{h}_{\mathrm{u}}^{\mathrm{H}}\left(\boldsymbol{I}-\boldsymbol{u}_{\mathrm{s}}\boldsymbol{u}_{\mathrm{s}}^{\mathrm{H}}\right)\boldsymbol{h}_{\mathrm{u}}\Bigg]\geq\alpha,\\&\quad\mathrm{tr}\left(\boldsymbol{B}\right)\leq P_{\mathrm{d}},\ \boldsymbol{B}\succeq 0,\end{aligned} \tag{15}$$

where $\hat{\boldsymbol{v}}_{\mathrm{s}}=\boldsymbol{U}^{\mathrm{H}}\boldsymbol{v}_{\mathrm{s}}$ and $\hat{\boldsymbol{h}}_{\mathrm{d}}=\boldsymbol{U}^{\mathrm{H}}\boldsymbol{h}_{\mathrm{d}}^{*}$. Note that the variable in Problem (P2) is $\boldsymbol{B}$ while that in Problem (P1) is $\boldsymbol{Q}_{\mathrm{d}}$. Once Problem (P2) is solved, $\boldsymbol{Q}_{\mathrm{d}}$ can be reconstructed by Eq. (14). In other words, Problem (P2) is equivalent to Problem (P1) when $\boldsymbol{H}_{\mathrm{s}}$ is a rank-one matrix.

To simplify Problem (P2), we discuss it with different values of α. When $R_{\mathrm{u}}^{\mathrm{L}}<\alpha\leq R_{\mathrm{u}}^{\mathrm{U}}$, Problem (P2) can be rewritten as

$$\begin{aligned}(\mathrm{P2.1})\ &\max_{\{\boldsymbol{B}\}}\ \log\left(1+\hat{\boldsymbol{h}}_{\mathrm{d}}^{\mathrm{H}}\boldsymbol{B}\hat{\boldsymbol{h}}_{\mathrm{d}}/N_0\right)\\ \mathrm{s.t.}\ &\lambda^2\hat{\boldsymbol{v}}_{\mathrm{s}}^{\mathrm{H}}\boldsymbol{B}\hat{\boldsymbol{v}}_{\mathrm{s}}\leq f(\alpha),\ \mathrm{tr}\left(\boldsymbol{B}\right)\leq P_{\mathrm{d}},\ \boldsymbol{B}\succeq 0,\end{aligned} \tag{16}$$

where

$$f(\alpha)=\frac{P_{\mathrm{u}}\boldsymbol{h}_{\mathrm{u}}^{\mathrm{H}}(\boldsymbol{u}_{\mathrm{s}}\boldsymbol{u}_{\mathrm{s}}^{\mathrm{H}})\boldsymbol{h}_{\mathrm{u}}}{2^{\alpha}-1-\frac{P_{\mathrm{u}}}{N_0}\boldsymbol{h}_{\mathrm{u}}^{\mathrm{H}}(\boldsymbol{I}-\boldsymbol{u}_{\mathrm{s}}\boldsymbol{u}_{\mathrm{s}}^{\mathrm{H}})\boldsymbol{h}_{\mathrm{u}}}-N_0\geq 0. \tag{17}$$

It is easy to check that Problem (P2.1) is concave and can be solved by standard convex optimization tools, e.g., CVX (http://cvxr.com/cvx). Then the rate pairs on the boundary of the achievable rate region with $R_{\mathrm{u}}^{\mathrm{L}}<\alpha\leq R_{\mathrm{u}}^{\mathrm{U}}$, can be obtained by solving Problem (P2.1).

In addition, if α is greater than $R_{\mathrm{u}}^{\mathrm{U}}$, the feasible set of Problem (P2) is empty due to its constraint of the UL rate. If $\alpha \leq R_{\mathrm{u}}^{\mathrm{L}}$, the constraint of the UL rate always holds, and the optimal DL rate β for Problem (P2) is $R_{\mathrm{d}}^{\mathrm{U}}$ defined in Eq. (4).

Therefore, there are two corner points on the boundary of the achievable rate region defined in Eq. (7), when α is equal to $R_{\mathrm{u}}^{\mathrm{L}}$ or $R_{\mathrm{u}}^{\mathrm{U}}$. When $\alpha = R_{\mathrm{u}}^{\mathrm{L}}$, the corresponding corner point on the boundary of the achievable rate region is $(R_{\mathrm{u}}^{\mathrm{L}}, R_{\mathrm{d}}^{\mathrm{U}})$. When $\alpha = R_{\mathrm{u}}^{\mathrm{U}}$, the corresponding optimal DL rate, which is denoted as $R_{\mathrm{d}}^{\mathrm{L}}$, is obtained by solving Problem (P2.1) with $\alpha = R_{\mathrm{u}}^{\mathrm{U}}$. Then the second corner point on the boundary of the achievable rate region is $(R_{\mathrm{u}}^{\mathrm{U}}, R_{\mathrm{d}}^{\mathrm{L}})$.

To sum up, the evaluation procedure to characterize the achievable rate region for the considered system under the case in which the SI channel is strongly correlated is illustrated in Algorithm 1. Note that δ_α is a small positive constant to control the density of all the obtained rate pairs.

Algorithm 1 Characterization of the achievable rate region for the considered system under the strongly correlated SI channel case

Initialize: $\alpha = 0$
while $\alpha \leq R_{\mathrm{u}}^{\mathrm{U}}$ **do**
  if $\alpha \leq R_{\mathrm{u}}^{\mathrm{L}}$ **then**
    The corresponding rate pair is $(\alpha, R_{\mathrm{d}}^{\mathrm{U}})$
  else
    Solve Problem (P2.1) with CVX to obtain (α, β).
  end if
  Update α: $\alpha \Leftarrow \alpha + \delta_\alpha$
end while
All the obtained rate pairs depict the boundary of the achievable rate region

3.3 Approximation to the general self-interference channel case

With some approximations, the proposed scheme can also be applied to the general SI channel case, i.e., the scenario that the SI channel matrix $\boldsymbol{H}_{\mathrm{s}}$ is of the rank more than 1. To begin with, define $N_{\min} = \min\{N_{\mathrm{T}}, N_{\mathrm{R}}\}$ and let the SVD of $\boldsymbol{H}_{\mathrm{s}}$ be

$$\boldsymbol{H}_{\mathrm{s}} = \boldsymbol{U}_{\mathrm{s}} \boldsymbol{\Sigma}_{\mathrm{s}} \boldsymbol{V}_{\mathrm{s}}^{\mathrm{H}}, \tag{18}$$

where $\boldsymbol{U}_{\mathrm{s}} \in \mathbb{C}^{N_{\mathrm{R}} \times N_{\min}}$, $\boldsymbol{V}_{\mathrm{s}} \in \mathbb{C}^{N_{\min} \times N_{\mathrm{T}}}$, and $\boldsymbol{\Sigma}_{\mathrm{s}} = \mathrm{diag}\,(\sigma_1, \sigma_2, \cdots \sigma_{N_{\min}})$ with its ith diagonal element being the ith maximum singular value of $\boldsymbol{H}_{\mathrm{s}}$. Then approximate $\boldsymbol{\Sigma}_{\mathrm{s}}$ by $\boldsymbol{\Sigma}'_{\mathrm{s}}$, where $\boldsymbol{\Sigma}_{\mathrm{s}} = \mathrm{diag}\,(\sigma_1, 0, \cdots 0)$. By adopting

$$\boldsymbol{H}'_s = \boldsymbol{U}_s \boldsymbol{\Sigma}'_s \boldsymbol{V}_s^{\mathrm{H}}, \tag{19}$$

we can approximately characterize the achievable rate region for the considered system under the general SI channel case.

Since the alternative SI channel matrix is not equal to the original SI channel matrix, there exists performance loss to design optimal precoding by using the proposed scheme in the general SI channel case, and its numerical results are shown in Section 4.2.

3.4 Comparisons to existing schemes

Note that the precoding matrix obtained in Nguyen *et al.* (2013) is only a sub-optimal solution to the sum rate maximization problem, while the proposed scheme in this study is claimed to achieve the optimal performance in the strongly correlated SI channel case.

The complexity of the two schemes is briefly compared. In the proposed scheme, Problem (P2.1) is a semi-definite programming (SDP) problem (Boyd and Vandenberghe, 2004). If the commonly used interior-point method is taken, the computational complexity for solving Problem (P2.1) is $O(4^3)$, since $\boldsymbol{B}$ has four variables (Boyd and Vandenberghe, 2004). In contrast, the innermost iteration of the scheme in Nguyen *et al.* (2013) requires a matrix inversion and a matrix square root operation as well as many matrix multiplications, and each of them requires computation on the order of N_{T}^3, where N_{T} is the number of Tx antennas at the BS. In general, the complexity of the proposed scheme will be lower than that of the scheme in Nguyen *et al.* (2013) when the number of Tx antennas is larger than four.

4 Numerical results

In this section, the proposed scheme and the one in Nguyen *et al.* (2013) are compared by simulations. The entries of channel vectors $\boldsymbol{h}_{\mathrm{u}}$ and $\boldsymbol{h}_{\mathrm{d}}$ are chosen as independent and identically distributed (i.i.d.) complex Gaussian random variables with zero mean and unit variance, and the noise power N_0 is set as 1. In addition, the transmit powers at the BS and UL MU, i.e., P_{d} and P_{u}, are set as 40 dBm.

4.1 Strongly correlated self-interference channel

In this subsection, the achievable rate region for the considered system under the case in which the SI channel is strongly correlated is simulated. The BS is equipped with four Tx antennas and four Rx antennas. The channel matrix of the residual SI at the BS is generated as a rank-one matrix according to $\boldsymbol{H}_{\mathrm{s}} = \delta_{\mathrm{si}}\boldsymbol{u}'_{\mathrm{s}}(\boldsymbol{v}'_{\mathrm{s}})^{\mathrm{H}}$, where both the entries of $\boldsymbol{u}'_{\mathrm{s}}$ and $\boldsymbol{v}'_{\mathrm{s}}$ are i.i.d. complex Gaussian random variables with zero mean and unit variance, and δ^2_{si} represents the average power of the residual SI.

Given a random strongly correlated SI channel realization, Fig. 2 depicts the achievable rate regions by exploiting the proposed scheme under different residual SI powers. Considering that the power of severe SI is greatly reduced after adopting the existing SI cancellation methods, the residual SI is assumed weak and its average power is respectively set as -5, 0, 5 dB in the simulation. It is observed that the achievable rate region becomes larger as δ^2_{si} decreases. It is due to the fact that when δ^2_{si} decreases, the power of the residual SI at the BS decreases, and thus the performance loss induced by the residual SI is reduced. Moreover, as δ^2_{si} decreases infinitely, the achievable rate region is asymptotically approaching its upper bound depicted by a dashed line, which is in the case of no residual SI.

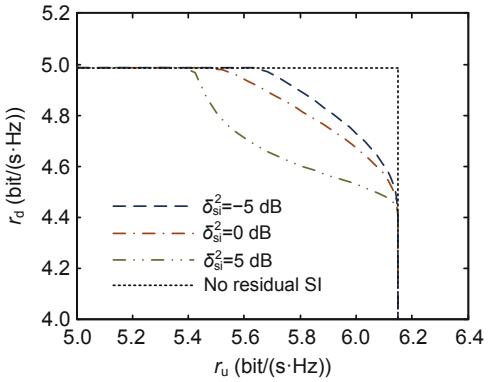

Fig. 2 Achievable rate regions characterized by the proposed scheme under a random strongly correlated self-interference channel realization

Figs. 3 and 4 show the achievable rate regions characterized by the proposed scheme as well as the rate pairs evaluated by the scheme in Nguyen *et al.* (2013) under four different random channel realizations with $\delta^2_{\mathrm{si}} = 3$ dB. Note that the rate pairs evaluated by the scheme in Nguyen *et al.* (2013) are marked as circles in the figures. Specifically, we focus on the right upper portion of the achievable rate region, which is sufficient to explain the performance difference between the two schemes. From the perspective of sum rate maximization, there exist two local maxima in the achievable rate region in each figure, and their corresponding sum rates are also labeled. It is observed from Fig. 3 that the sum rates evaluated by the scheme in Nguyen *et al.* (2013) are equal to the global maxima respectively, with 0.72 and 0.95 bits/(s·Hz) higher than the other local maxima. However, they are just local maxima in Fig. 4 respectively, with 1.35 and 0.36 bits/(s·Hz) lower than the global maxima. As a consequence, only a local optimum, which is not always the global optimum, is derived by using the scheme in Nguyen *et al.* (2013). Nevertheless, the optimal performance

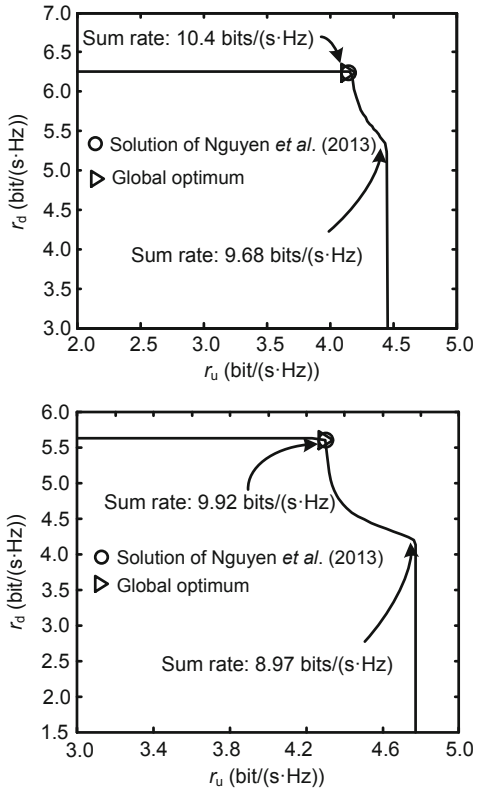

Fig. 3 Achievable rate regions calculated by using the proposed scheme, compared with the rate pairs evaluated by the scheme in Nguyen *et al.* (2013) under two different random strongly correlated SI channel realizations, where the sum rates evaluated by the scheme in Nguyen *et al.* (2013) are the optima

is achieved by exploiting the proposed scheme in this study.

4.2 General self-interference channel

In the general SI channel case, N_{T} and N_{R} are both set as two or four for simplification. Under the simulation condition of $N_{\mathrm{T}}=N_{\mathrm{R}}=2$, the eigenvalue ratio of the SI channel matrix $\boldsymbol{H}_{\mathrm{s}}\in\mathbb{C}^{2\times2}$ is defined as the ratio of the amplitude of its smaller eigenvalue to that of the larger one. When $N_{\mathrm{T}}=N_{\mathrm{R}}=4$, the amplitudes of the other three eigenvalues except the largest one are assumed to be identical, and the eigenvalue ratio of the SI channel matrix $\boldsymbol{H}_{\mathrm{s}}\in\mathbb{C}^{4\times4}$ is defined as the ratio of the identical amplitude of the other three eigenvalues to that of the largest one. A temporary matrix $\boldsymbol{J}\in\mathbb{C}^{N_{\mathrm{T}}\times N_{\mathrm{R}}}$, the entries of which are i.i.d. complex Gaussian random variables with zero mean and variance $\delta_{\mathrm{si}}^2=3$ dB, is generated by MATLAB. Then we perform eigenvalue decomposition on matrix $\boldsymbol{J}$, and regulate the amplitudes of its eigenvalues with the given eigenvalue ratio, to obtain the final SI matrix $\boldsymbol{H}_{\mathrm{s}}$.

Fig. 5 shows the approximate maximum sum rate found from the achievable rate region characterized by the proposed scheme, compared with the global maximum sum rate obtained by the exhaustive search as well as the local maximum one evaluated by the scheme in Nguyen *et al.* (2013). It is observed that the sum rate loss of the proposed scheme increases along with the eigenvalue ratio's growth. In detail, even when the eigenvalue ratio is 1, the sum rate loss of the proposed scheme relative to the global maximum is no more than 0.5 bits/(s·Hz) under the channel realization when $N_{\mathrm{T}}=N_{\mathrm{R}}=2$ (Fig. 5a), and it is almost 1 bit/(s·Hz) under the channel realization when $N_{\mathrm{T}}=N_{\mathrm{R}}=4$ (Fig. 5b). Furthermore,

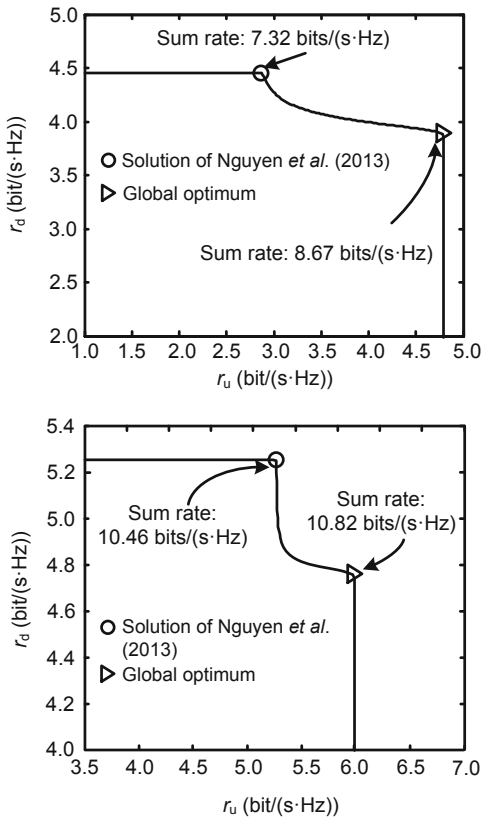

Fig. 4 Achievable rate regions calculated by using the proposed scheme, compared with the rate pairs evaluated by the scheme in Nguyen *et al.* (2013) under two different random strongly correlated SI channel realizations, where the sum rates evaluated by the scheme in Nguyen *et al.* (2013) are not the optima

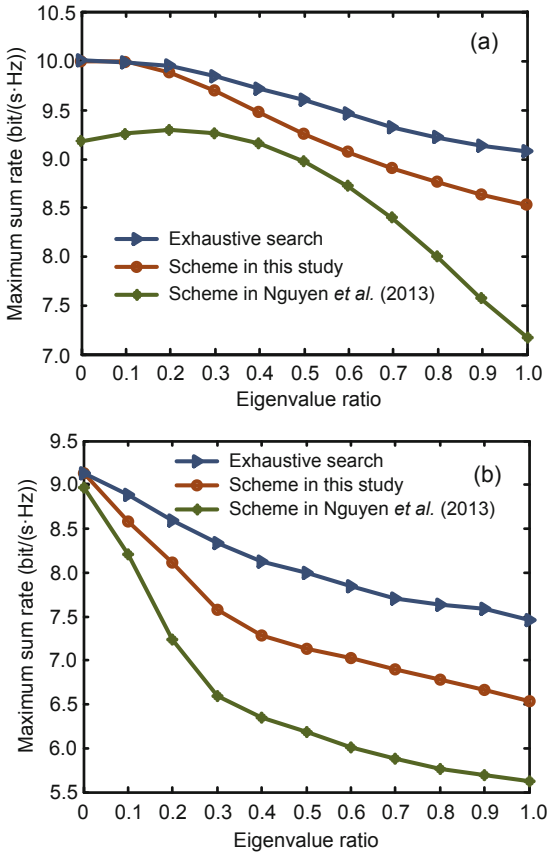

Fig. 5 Evaluated maximum sum rates under different eigenvalue ratios by using the exhaustive search (global optimal solutions), the proposed scheme in this study, and the scheme proposed by Nguyen *et al.* (2013): (a) $N_{\mathrm{T}}=N_{\mathrm{R}}=2$; (b) $N_{\mathrm{T}}=N_{\mathrm{R}}=4$

the performance of the proposed scheme is better than that of the scheme in Nguyen *et al.* (2013).

5 Conclusions

We have investigated the optimal precoding for an FD cellular system in the strongly correlated SI channel case. The non-convex DL rate maximization problem subject to a targeted UL rate was adopted to characterize the achievable rate region for the considered system. Considering the strongly correlated property of the SI channel, the original problem was transformed into a convex problem, and solved by the standard convex optimization tools. Then the achievable rate region for this FD cellular system was derived by solving a sequence of the DL rate maximization problems with different targeted UL rates. Compared to the precoding design in Nguyen *et al.* (2013), which offered a sub-optimal solution, the proposed scheme achieved the optimal performance under the case in which the SI channel was strongly correlated. In addition, the proposed scheme was applied to the general SI channel case with some approximations.

References

Bharadia, D., McMilin, E., Katti, S., 2013. Full duplex radios. *ACM SIGCOMM Comput. Commun. Rev.*, **43**(4):375-386. http://dx.doi.org/10.1145/2486001.2486033

Boyd, S., Vandenberghe, L., 2004. Convex Optimization. Cambridge University Press, UK.

Cirik, A.C., 2015. Fairness considerations for full duplex multi-user MIMO systems. *IEEE Wirel. Commun. Lett.*, **4**(4):361-364. http://dx.doi.org/10.1109/LWC.2015.2419672

Cirik, A.C., Rong, Y., Hua, Y., 2014. Achievable rates of full-duplex MIMO radios in fast fading channels with imperfect channel estimation. *IEEE Trans. Signal Process.*, **62**(15):3874-3886. http://dx.doi.org/10.1109/TSP.2014.2330806

Haneda, K., Khatun, A., Dashti, M., *et al.*, 2013a. Measurement-based analysis of spatial degrees of freedom in multipath propagation channels. *IEEE Trans. Anten. Propag.*, **61**(2):890-900. http://dx.doi.org/10.1109/TAP.2012.2223431

Haneda, K., Khatun, A., Gustafson, C., *et al.*, 2013b. Spatial degrees-of-freedom of 60 GHz multiple-antenna channels. Proc. IEEE 77th Vehicular Technology Conf., p.1-5. http://dx.doi.org/10.1109/VTCSpring.2013.6692762

Huberman, S., Le-Ngoc, T., 2015. Full-duplex MIMO precoding for sum-rate maximization with sequential convex programming. *IEEE Trans. Veh. Technol.*, **64**(11):5103-5112. http://dx.doi.org/10.1109/TVT.2014.2380775

Nguyen, D., Tran, L.N., Pirinen, P., *et al.*, 2013. Precoding for full duplex multiuser MIMO systems: spectral and energy efficiency maximization. *IEEE Trans. Signal Process.*, **61**(16):4038-4050. http://dx.doi.org/10.1109/TSP.2013.2267738

Nguyen, D., Tran, L.N., Pirinen, P., *et al.*, 2014. On the spectral efficiency of full-duplex small cell wireless systems. *IEEE Trans. Wirel. Commun.*, **13**(9):4896-4910. http://dx.doi.org/10.1109/TWC.2014.2334610

Pu, X., Shao, S., Deng, K., *et al.*, 2015. Effects of array orientations on degrees of freedom for 3D LoS channels in short-range communications. *IEEE Wirel. Commun. Lett.*, **4**(1):106-109. http://dx.doi.org/10.1109/LWC.2014.2381221

Sabharwal, A., Schniter, P., Guo, D., *et al.*, 2014. In-band full-duplex wireless: challenges and opportunities. *IEEE J. Sel. Areas Commun.*, **32**(9):1637-1652. http://dx.doi.org/10.1109/JSAC.2014.2330193

Yousif, E.H.G., Ratnarajah, T., Sellathurai, M., 2015. Modeling and performance analysis of multitaper detection using phase-type distributions over MIMO fading channels. *IEEE Trans. Signal Process.*, **63**(22):5882-5896. http://dx.doi.org/10.1109/TSP.2015.2455520

Zhang, R., Liang, Y.C., Chai, C.C., *et al.*, 2009. Optimal beamforming for two-way multi-antenna relay channel with analogue network coding. *IEEE J. Sel. Areas Commun.*, **27**(5):699-712. http://dx.doi.org/10.1109/JSAC.2009.090611

Appendix A: Proof of Proposition 1

Considering the fact that the SI channel matrix is of rank one, i.e., $\boldsymbol{H}_{\mathrm{s}}=\lambda\boldsymbol{u}_{\mathrm{s}}\boldsymbol{v}_{\mathrm{s}}^{\mathrm{H}}$, R_{u} can be rewritten as

$$R_{\mathrm{u}}=\log\left[1+P_{\mathrm{u}}\boldsymbol{h}_{\mathrm{u}}^{\mathrm{H}}(N_0\boldsymbol{I}+\lambda^2\boldsymbol{u}_{\mathrm{s}}\boldsymbol{v}_{\mathrm{s}}^{\mathrm{H}}\boldsymbol{Q}_{\mathrm{d}}\boldsymbol{v}_{\mathrm{s}}\boldsymbol{u}_{\mathrm{s}}^{\mathrm{H}})^{-1}\boldsymbol{h}_{\mathrm{u}}\right]. \tag{A1}$$

Define a unitary matrix $\boldsymbol{U}_{\mathrm{s}}$, the first column of which is $\boldsymbol{u}_{\mathrm{s}}$. Then $\boldsymbol{M}=(N_0\boldsymbol{I}+\lambda^2\boldsymbol{u}_{\mathrm{s}}\boldsymbol{v}_{\mathrm{s}}^{\mathrm{H}}\boldsymbol{Q}_{\mathrm{d}}\boldsymbol{v}_{\mathrm{s}}\boldsymbol{u}_{\mathrm{s}}^{\mathrm{H}})^{-1}$ can be shown equal to

$$\boldsymbol{M}=\boldsymbol{U}_{\mathrm{s}}\begin{bmatrix}\dfrac{1}{N_0+\lambda^2\boldsymbol{v}_{\mathrm{s}}^{\mathrm{H}}\boldsymbol{Q}_{\mathrm{d}}\boldsymbol{v}_{\mathrm{s}}} & & & \\ & \dfrac{1}{N_0} & & \\ & & \ddots & \\ & & & \dfrac{1}{N_0}\end{bmatrix}\boldsymbol{U}_{\mathrm{s}}^{\mathrm{H}}. \tag{A2}$$

After simplification, R_{u} becomes Eq. (10), which completes the proof.

Appendix B: Proof of Proposition 2

To begin with, a unitary matrix $[\boldsymbol{U},\boldsymbol{U}^{\perp}]^{N_{\mathrm{T}}\times N_{\mathrm{T}}}$ is introduced, where $\boldsymbol{U}$ is given in Eq. (13) and

$\boldsymbol{U}^{\perp}(\boldsymbol{U}^{\perp})^{\mathrm{H}} = \boldsymbol{I} - \boldsymbol{U}\boldsymbol{U}^{\mathrm{H}}$. Without loss of generality, $\boldsymbol{Q}_{\mathrm{d}}$ can be expressed as

$$\begin{aligned}\boldsymbol{Q}_{\mathrm{d}} &= [\boldsymbol{U}, \boldsymbol{U}^{\perp}] \begin{bmatrix} \boldsymbol{B} & \boldsymbol{C} \\ \boldsymbol{D} & \boldsymbol{E} \end{bmatrix} [\boldsymbol{U}, \boldsymbol{U}^{\perp}]^{\mathrm{H}} \\ &= \boldsymbol{U}\boldsymbol{B}\boldsymbol{U}^{\mathrm{H}} + \boldsymbol{U}\boldsymbol{C}(\boldsymbol{U}^{\perp})^{\mathrm{H}} \\ &\quad + \boldsymbol{U}^{\perp}\boldsymbol{D}\boldsymbol{U}^{\mathrm{H}} + \boldsymbol{U}^{\perp}\boldsymbol{E}(\boldsymbol{U}^{\perp})^{\mathrm{H}},\end{aligned} \tag{B1}$$

where $\boldsymbol{B} \in \mathbb{C}^{2\times 2}$, $\boldsymbol{C} \in \mathbb{C}^{2\times(N_{\mathrm{T}}-2)}$, $\boldsymbol{D} \in \mathbb{C}^{(N_{\mathrm{T}}-2)\times 2}$, and $\boldsymbol{E} \in \mathbb{C}^{(N_{\mathrm{T}}-2)\times(N_{\mathrm{T}}-2)}$.

Recall that $\boldsymbol{U}$ is spanned by $\boldsymbol{v}_{\mathrm{s}}$ and $\boldsymbol{h}_{\mathrm{d}}^{*}$, and thus all columns in $\boldsymbol{U}^{\perp}$ are, respectively, linearly independent of $\boldsymbol{v}_{\mathrm{s}}$ and $\boldsymbol{h}_{\mathrm{d}}^{*}$. Therefore, the two terms, $\boldsymbol{h}_{\mathrm{d}}^{\mathrm{T}}\boldsymbol{Q}_{\mathrm{d}}\boldsymbol{h}_{\mathrm{d}}^{*}$ in Eq. (2) and $\boldsymbol{v}_{\mathrm{s}}^{\mathrm{H}}\boldsymbol{Q}_{\mathrm{d}}\boldsymbol{v}_{\mathrm{s}}$ in Eq. (10), are simplified as $\boldsymbol{h}_{\mathrm{d}}^{\mathrm{T}}\boldsymbol{U}\boldsymbol{B}\boldsymbol{U}^{\mathrm{H}}\boldsymbol{h}_{\mathrm{d}}^{*}$ and $\boldsymbol{v}_{\mathrm{s}}^{\mathrm{H}}\boldsymbol{U}\boldsymbol{B}\boldsymbol{U}^{\mathrm{H}}\boldsymbol{v}_{\mathrm{s}}$, respectively. Since R_{d} and R_{u} are given in Eqs. (2) and (10) respectively, they are independent of $\boldsymbol{C}$, $\boldsymbol{D}$, and $\boldsymbol{E}$. In addition, referring to $\boldsymbol{Q}_{\mathrm{d}}$ being a positive semi-definite matrix and $\mathrm{tr}(\boldsymbol{Q}_{\mathrm{d}}) = \mathrm{tr}(\boldsymbol{B}) + \mathrm{tr}(\boldsymbol{E})$, $\mathrm{tr}(\boldsymbol{B}) \geq 0$ and $\mathrm{tr}(\boldsymbol{E}) \geq 0$ are derived, and then the power constraint $\mathrm{tr}\,(\boldsymbol{Q}_{\mathrm{d}}) \leq P_{\mathrm{d}}$ in Problem (P1) can be relaxed as $\mathrm{tr}\,(\boldsymbol{B}) \leq P_{\mathrm{d}}$. From the above, Problem (P1) has no relationship with $\boldsymbol{C}$, $\boldsymbol{D}$, or $\boldsymbol{E}$. Thus, $\boldsymbol{Q}_{\mathrm{d}} = \boldsymbol{U}\boldsymbol{B}\boldsymbol{U}^{\mathrm{H}}$ is concluded.